International Journal of Neuropsychopharmacology (2017) 00(00): 1–13

doi:10.1093/ijnp/pyx096
Advance Access Publication: November 1, 2017
Regular Research Article

REGULAR RESEARCH ARTICLE

NYX-2925 Is a Novel NMDA Receptor-Specific Spirocyclic-β-Lactam That Modulates Synaptic Plasticity Processes Associated with Learning and Memory

M. Amin Khan, David R. Houck, Amanda L. Gross, Xiao-lei Zhang, Cassia Cearley, Torsten M. Madsen, Roger A. Kroes, Patric K. Stanton, Jeffrey Burgdorf, Joseph R. Moskal

Aptinyx Inc., Evanston, Ilinois (Drs Khan, Houck, Gross, Cearley, Madsen, Kroes, Burgdorf, and Moskal); Department of Cell Biology & Anatomy, New York Medical College, Valhalla, New York (Drs Zhang and Stanton); Falk Center for Molecular Therapeutics, Department of Biomedical Engineering, Northwestern University, Evanston, Ilinois (Drs Kroes, Burgdorf, and Moskal).

Correspondence: Joseph Moskal, PhD, Falk Center for Molecular Therapeutics, Northwestern University Department of Biomedical Engineering, 1801 Maple Ave, Suite 4300, Evanston, IL, 60201 (j-moskal@northwestern.edu).

Abstract

Background: N-methyl-D-aspartate receptors are one member of a family of ionotropic glutamate receptors that play a pivotal role in synaptic plasticity processes associated with learning and have become attractive therapeutic targets for diseases such as depression, anxiety, schizophrenia, and neuropathic pain. NYX-2925 ((2S, 3R)-3-hydroxy-2-((R)-5-isobutyryl-1-oxo-2,5-diazaspiro[3.4]octan-2-yl)butanamide) is one member of a spiro-β-lactam-based chemical platform that mimics some of the dipyrrolidine structural features of rapastinel (formerly GLYX-13: threonine-proline-proline-threonine) and is distinct from known N-methyl-D-aspartate receptor agonists or antagonists such as D-cycloserine, ketamine, MK-801, kynurenic acid, or ifenprodil.

Methods: The in vitro and in vivo pharmacological properties of NYX-2925 were examined.

Results: NYX-2925 has a low potential for "off-target" activity, as it did not exhibit any significant affinity for a large panel of neuroactive receptors, including hERG receptors. NYX-2925 increased MK-801 binding to human N-methyl-D-aspartate receptor NR2A-D subtypes expressed in HEK cells and enhanced N-methyl-D-aspartate receptor current and long-term potentiation (LTP) in rat hippocampal slices (100–500 nM). Single dose ex vivo studies showed increased metaplasticity in a hippocampal LTP paradigm and structural plasticity 24 hours after administration (1 mg/kg p.o.). Significant learning enhancement in both novel object recognition and positive emotional learning paradigms were observed (0.01–1 mg/kg p.o.), and these effects were blocked by the N-methyl-D-aspartate receptor antagonist CPP. NYX-2925 does not show any addictive or sedative/ataxic side effects and has a therapeutic index of >1000. NYX-2925 (1 mg/kg p.o.) has a cerebrospinal fluid half-life of 1.2 hours with a Cmax of 44 nM at 1 hour.

Conclusions: NYX-2925, like rapastinel, activates an NMDA receptor-mediated synaptic plasticity process and may have therapeutic potential for a variety of NMDA receptor-mediated central nervous system disorders.

Keywords: NMDA receptor, learning and memory, synaptic plasticity

Received: August 2, 2017; **Revised:** October 7, 2017; **Accepted:** October 17, 2017

Significance Statement

NYX-2925 is a novel NMDA receptor-specific modulator that facilitates synaptic plasticity and has therapeutic potential for a variety of NMDA receptor-mediated central nervous system (CNS) disorders. NYX-2925 was synthesized using a novel spirocyclic-β-lactam chemical approach using rapastinel (formerly GLYX-13) as a template, which was in turn synthesized from a hypervariable region of a unique monoclonal antibody with NMDA receptor modulatory properties. Thus, the creation of NYX-2925 completes the process of developing monoclonal antibodies to help elucidate the molecular mechanisms of complex biological processes such as learning and memory and converting them into small molecules with therapeutic potential.

Introduction

N-methyl-D-aspartate (NMDA) receptors are one of a family of ligand gated ionotropic glutamate receptors that are found predominantly in the CNS and developmentally regulated (Cull-Candy et al., 2001; Traynelis et al., 2010). They are unique among glutamate receptors in that they require both glutamate and glycine for full activation (Danysz and Parsons, 1998). They are heterotetrameric complexes that are expressed as multiple subtypes each with unique properties (Paoletti et al., 2013). NMDA receptors play a pivotal role in modulating normal neuronal functions including activity-dependent synaptic plasticity associated with learning and memory (Bliss and Collingridge, 1993; Yashiro and Philpot, 2008; Morris, 2013) and have been implicated in a variety of CNS disorders, including schizophrenia (Coyle, 2012; Goff, 2012), mood disorders (Ghasemi et al., 2014; Vasilescu et al., 2017), epilepsy (Ghasemi and Schachter, 2011), neuropathic pain (Millecamps et al., 2007; Zhou et al., 2011), fibromyalgia (Harris et al., 2008; Pyke et al., 2016), Rett syndrome (Patrizi et al., 2016), and cognitive decline due to normal aging (Robb, 1991; Burgdorf et al., 2011a) among others.

Recently, reports have described positive clinical trial data with mechanistically distinct NMDA receptor modulators including rapastinel (formerly GLYX-13) and ketamine for depression (Fond et al., 2014; Preskorn et al., 2015) and obsessive-compulsive disorder (Rodriguez et al., 2013, 2016), D-cycloserine for schizophrenia (Cain et al., 2014) and posttraumatic stress disorder (de Kleine et al., 2012), and memantine for Alzheimer's disease (Wilkinson et al., 2014). The key role that NMDA receptors play in synaptic plasticity throughout the CNS, the marked increase in NMDA receptor mechanistic studies, including X-ray crystallographic analysis (Karakas and Furukawa, 2014; Dolino et al., 2015; Lu et al., 2017), and biophysical studies on receptor subtype properties (Tavoloni and Schaffner, 1989; Iacobucci and Popescu, 2017), coupled with clinical trial successes seen with NMDA receptor modulators, make this receptor complex an attractive target for drug discovery.

Rapastinel is a tetrapeptide (threonine-proline-proline-threonine) derived from a hypervariable region of a monoclonal antibody B6B21 (Moskal et al., 2005). B6B21 was shown to act as a cognitive enhancer (Thompson et al., 1992) with glycine-site partial agonist properties at the NMDA receptor (Haring et al., 1991). Rapastinel has also been found to be a robust cognitive enhancer with marked antidepressant-like effects in a variety of rat models (Burgdorf et al., 2013, 2017). Mechanistically, rapastinel appears to bind directly to NMDA receptors, triggering an increase in AMPA receptor activity and leading to a long-term potentiation-like increase in synaptic plasticity associated with learning (Moskal et al., 2017).

A key structural feature of rapastinel is its dipyrrolidine-based β-turn motif. A novel chemical platform was created using spirocyclic-β-lactam chemistry (Bittermann and Gmeiner, 2006) with a variety of NMDA receptor subtype selectivity, potency, and activity profiles. NYX-2925 is a representative compound from this platform. Figure 1 shows the structure of rapastinel and NYX-2925, and we report on its pharmacological, toxicological, functional, and mechanistic properties.

Materials and Methods

Animals

Adult male Sprague-Dawley rats from Harlan or Charles River were used for most studies. For the novel object recognition study, adult male Lister Hooded rats from Harlan were used. Rats were group housed (3–4 per cage) in Lucite cages with aspen wood chip bedding, maintained on a 12-hour-light/12-hour-dark cycle (lights on at 5:00 AM), and given ad libitum access to Purina Lab Chow and tap water throughout the study. For the drug discrimination study, rats were singly housed with ad libitum access to water. All experiments were approved by the Northwestern University, Virginia Commonwealth University, and New York Medical College Institutional Animal Care and Use Committees.

Drugs

NYX-2925 was synthesized by Sai Life Sciences (India) and was administered p.o. (0.1–10 mg/kg) in 1 mL/kg in 0.5% carboxymethylcellulose (CMC) 0.9% sterile saline. The NMDA receptor glutamate site antagonist CPP ((±)-3-(2-carboxypiperazin-4-yl) propyl-1-phosphonic acid) was purchased from Sigma and administered i.p. (10 mg/kg) in 1 mL/kg 0.9% sterile saline. The dose of CPP (10 mg/kg i.p.) was chosen based on previous reports that this dose could block the antidepressant-like effects of an NMDAR positive modulator without exhibiting behavioral effects on its own (L. Zhang et al., 2013; Burgdorf et al., 2015b). The 5-HT_6 receptor antagonist SB399885 was purchased from GVK Biosciences (India) and was administered p.o. (10 mg/kg) in 2 mL/kg 1% CMC and was used as a positive control in the novel object recognition study (Hirst et al., 2006). Ketamine-HCl (Ketalar) was obtained from Patterson Veterinary Inc. and was diluted with 0.9 % saline to the concentration required to provide the desired dose in a 1-mL/kg volume for both i.p. and p.o. administration.

[^{3}H] MK-801 Potentiation Assay

NMDAR Subtype Expressing HEK Cell Membrane Preparation

Crude membranes were prepared using transiently transfected, NMDAR-expressing HEK cells, described below. All procedures were performed at 4°C. Briefly, pelleted cells were initially washed in 10 mM Tris acetate (pH 7.4 at 4°C), pelleted, and frozen at -80°C overnight. The pellet was then resuspended and homogenized (30 strokes) in a glass homogenizer and pelleted at 51 500 x g for 30 minutes at 4°C and stored at –80°C until assay.

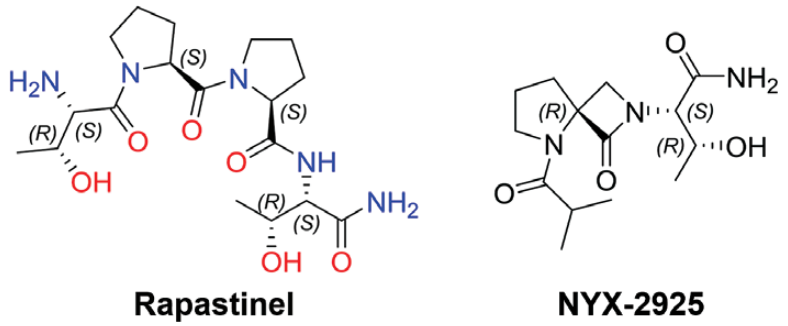

Figure 1. Structural comparison of the peptide rapastinel with the spirocyclic β-lactam, ((2S, 3R)-3-hydroxy-2-((R)-5-isobutyryl-1-oxo-2,5-diazaspiro[3.4]octan-2-yl) butanamide) (NYX-2925). Spirocyclic β-lactam chemistry has been used to create a number of new molecules that mimic key properties of their parent peptides (Bittermann and Gmeiner, 2006).

Functional glycine site agonist effects were measured using an [^{3}H] MK-801 potentiation assay. Briefly, 300 μg of membrane extract protein were preincubated for 15 minutes at 25°C in the presence of a saturating concentration of glutamate (50 μM) and varying concentrations of NYX-2925. Following the addition of 0.3mCi [^{3}H] MK-801 (Amersham, 22.5 Ci/mmol), reactions were incubated for an additional 15 minutes (nonequilibrium conditions). Bound and free [^{3}H] MK-801 were separated via rapid filtration. Zero levels were determined in the absence of any glycine ligand. The percent maximal [^{3}H] MK-801 binding was calculated relative to stimulation measured in the presence of 1 mM glycine and 50 μM glutamate. Binding curves were fitted using GraphPad software.

Creation of the Stable hNMDAR1-Expressing HEK Cell Line

The cDNA encoding the human GluN1-1 (GenBank BC156961) was amplified from MGC clone 100063609 using pfu polymerase and subcloned into the pCMV/zeoDNA3 vector using standard molecular techniques and verified by direct sequencing. HEK cells (ATCC) were transfected with the mutant construct using X-tremeGENE 9 transfection reagent (Roche) and stable clones selected in Zeocin-containing media.

Creation of the Transient hNMDAR2 (A-D) Expression Vectors

cDNAs encoding the hNMDAR2A (GENBANK #NM_000833, pfu polymerase amplified from human cortex cDNA), hNMDAR2B (GENBANK #NM_000834, pfu polymerase amplified from Open Systems clone #8322670), hNMDAR2C (GENBANK #NM_000835, pfu polymerase amplified from OriGene clone #SC300138), and hNMDAR2D (GENBANK #NM_000836, pfu polymerase amplified from OriGene clone #SC300139) were subcloned into the pCMV6/XL5 vector using standard molecular techniques.

Off-Target Receptor Binding Assays

To further characterize the target specificity of NYX-2925, we tested the ability of 10 μM NYX-2925 (>10 000 × Cmax) to compete for binding in a radioligand displacement assay using a broad panel of known CNS protein targets (LeadProfilingScreen 2, Eurofins Cerep). The binding panel included adenosine and adrenergic receptor sites; dopamine, histamine, and opioid receptors; calcium channels; and muscarinic cholinergic receptor sites.

Bioavailability

Male Sprague Dawley rats were dosed with NYX-2925 (1 mg/kg p.o.), and jugular vein blood draws taken in K2-EDTA-treated tubes and cisterna magna cerebrospinal fluid (CSF) draws were taken at various time points. Samples were maintained at 4°C for 30 to 60 minutes after collection and stored at 80°C until assay. On the day of the assay, plasma, CSF, and standards were thawed at 4°C. Samples were extracted with acetonitrile and NYX-2925 levels were assessed by liquid chromatography tandem mass spectrometry and the lower limit of quantification for this assay was ~4 nM.

Dendritic Spine Morphology Analysis

Dendritic spine analyses were conducted as previously described (Ota et al., 2014; Burgdorf et al., 2015b) using the Afraxis ESP Platform (Afraxis, Inc.). Animals were given a single dose of NYX-2925 (1 mg/kg p.o.), or 0.5% Na-CMC in 0.9% sterile saline vehicle (1 mL/kg), and 24 hours post dosing they were deeply anesthetized (isoflurane) and brains fixed via cardiac perfusion using 4% paraformaldehyde. Brains were stored in ice cold 0.1 M phosphate buffer and stored at 4°C until sectioning. Brains were sectioned using a Vibratome (Leica VT1000) to collect sections (300 μm thick) from the anterior to posterior extremes of each brain. Ballistic dye labeling (DiI and DiO; 3 mg dissolved in methylene chloride and coated on tungsten particles) was performed using a commercially available gene gun (Bio-Rad) to label neurons. Thick sections were mounted to slides with raised barriers using ProLong Gold (Life Technologies) and cover slipped. Laser-scanning confocal microscopy (Olympus FV1000) was performed using a 63 × objective (1.42 NA) to scan individually labeled neurons at high resolution (0.103 × 0.103 × 0.33 μm voxels). Microscopy was performed blind to experimental conditions. A minimum of 5 cells per animal were sampled. Primary dendrites within the inner molecular layer were analyzed, and samples (50 μm) were collected from primary dendrites starting at 100 μm from the soma. Spine head and neck sizes were analyzed given that larger spine head and necks are associated with greater NMDAR-mediated calcium flux (Noguchi et al., 2005) as well as the induction of LTP (Matsuzaki et al., 2004).

Blind deconvolution (AutoQuant) was applied to raw 3-dimensional digital images that were then analyzed for spine density and morphology by trained analysts. Individual spines were measured manually for (a) head diameter, (b) spine length, and (c) spine neck diameter from image Z-stacks using software custom-designed by Afraxis Inc. Each dendrite was analyzed by 3 to 4 independent analysts. Analysts were blinded

to all experimental conditions (including treatment, brain region, and cell type).

Extracellular Hippocampal Recordings

Experiments were conducted as described previously (Zhang et al., 2008; Burgdorf et al., 2015b). Adult male rats were deeply anesthetized with isoflurane and decapitated. Brains were removed rapidly, submerged in ice-cold artificial CSF (ACSF, 2–4°C), which contained (in mM): 124 NaCl, 4 KCl, 1.5 $MgCl_2$, 2.5 $CaCl_2$, 1.25 NaH_2PO_4, 26 $NaHCO_3$, 10 glucose; at pH 7.4, gassed continuously with 95% O_2/5% CO_2. Brains were hemisected, the frontal lobes removed, and individual hemispheres glued using cyanoacrylate adhesive onto a stage immersed in ice-cold ACSF gassed continuously with 95% O_2/5% CO_2 during slicing. Then 400-µm-thick coronal slices were cut using a Vibratome (Leica VT1200S) and transferred to an interface holding chamber for incubation at room temperature for a minimum of 1 hour before transferring to a Haas-style interface recording chamber continuously perfused at 3 mL/min with oxygenated ACSF at 32 ± 0.5°C.

Low resistance recording electrodes were made from thin-walled borosilicate glass (1–2 MΩ after filling with ACSF) and inserted into the apical dendritic region of the Schaffer collateral termination field in stratum radiatum of the CA1 region to record field excitatory postsynaptic potentials (fEPSPs). A bipolar stainless-steel stimulating electrode (FHC) was placed on Schaffer collateral-commissural fibers in CA3 stratum radiatum, and constant current stimulus intensity adjusted to evoke approximately half-maximal fEPSPs once each 30 seconds (50–100 pA; 100-µs duration). fEPSP slope was measured before and after induction of LTP or LTD by linear interpolation from 20% to 80% of maximum negative deflection, and slopes confirmed to be stable to within ± 10% for at least 15 minutes before commencing an experiment. Signals were recorded using a Multiclamp 700B amplifier and digitized with a Digidata 1322 (Axon Instruments). Data were analyzed using pClamp software (version 9, Axon Instruments).

Hippocampal LTP and LTD Studies

Experiments were conducted as described previously (Zhang et al., 2008). LTP was induced by 2 theta trains pared by 3 minutes (3 × 100 Hz/500 ms) and LTD induced by a low-frequency stimulus train (2 Hz/10 min). LTP/LTD was measured 40 minutes after high- or low-frequency stimulation. NYX-2925 was bath applied for 40 to 50 minutes starting 20 minutes before application of high- or low-frequency stimulation.

Medial Prefrontal Cortex (MPFC) LTP Studies

Experiments were conducted as described previously (Burgdorf et al., 2015a). Four-hundred-µm thick slices were cut using a vibratome (Leica VT1200S) in a modified coronal orientation (Parent et al., 2010) containing both prelimbic and infralimbic regions of the MPFC that are targets (via the fornix) of the hippocampal-MPFC pathway. Recording electrodes were inserted into layer III/IV of the prelimbic MPFC and monosynaptically evoked fEPSPs evoked by mixed excitatory inputs were recorded from layer V pyramidal neurons. A bipolar tungsten stimulating electrode (FHC) was placed on MPFC deep white matter. LTP was induced by stimulation of input axons with 3 high-frequency theta burst stimulus trains of 10 × 100 Hz/5 pulse bursts each, applied at an inter-burst interval of 200 milliseconds. Each train was 2 seconds in duration, and trains were applied 3 minutes apart. LTP/LTD was measured 40 minutes after high-frequency stimulation induction. NYX-2925 was bath applied for 40 to 50 minutes starting 20 minutes before application of high-frequency stimulation.

Metaplasticity Studies

Experiments were conducted as described previously (Burgdorf et al., 2015b). Rats were dosed with NYX-2925 (1 mg/kg p.o.) and hippocampal slices were prepared either 24 hours or 1 week post dosing. Three submaximal bouts of high-frequency Schaffer collateral stimulation (2 × 100 Hz/800 ms) were applied 20 minutes apart. LTP was measured 40 minutes after the last high-frequency bout of stimulation.

Intracellular Recordings from Hippocampal CA1 Pyramidal Neurons

Whole-cell patch clamp recordings from CA1 pyramidal neurons were acquired as described previously (Burgdorf et al., 2013). Patch pipette resistance was 6 to 6.5 MΩ when filled with intracellular solution that contained (in mM): 135 $CsMeSO_2$, 8 NaCl, 10 HEPES, 0.2 EGTA, 2 Mg-ATP, 0.3 Na-GTP, and 1 QX-314 [N-(2,6-dimethylphenylcarbamoylthyl)-triethylammonium bromide], 275 mOsm, pH 7.25 adjusted with $Cs(OH)_2$. CA1 pyramidal neurons were visualized by infrared imaging and patched using a 60x water-immersed objective mounted to a Zeiss microscope (Axioskop 2 Fs plus). After whole-cell voltage clamp configuration was established, access resistance was carefully monitored, and only cells with stable access resistance (<5% change) were included in analyses. Excitatory postsynaptic currents (EPSCs) were recorded using a MultiClamp 700B (Molecular Devices); with the low-pass filter setting at 1 to 3 kHz, series resistance was compensated in the voltage-clamp mode, and patched cells whose series resistance changed by >10% were rejected from analysis. Signals were filtered at 3 kHz and digitized at 10 kHz with a Digidata 1322A controlled by a Clampex (v9.2) (Molecular Devices). A bipolar tungsten stimulating electrode (FHC) was placed in the Schaffer collateral-commissural fibers in CA3 stratum radiatum and stimulus pulses (800 µS duration) were delivered at 15- to 30-second intervals. Neurons were voltage clamped at -70 mV to record EPSCs to assess input-output relations and paired-pulse facilitation. Neurons were clamped at -40 mV for recording NMDA currents to relieve voltage-dependent magnesium block, and slices were perfused with ACSF containing 0 added magnesium, 3 mM calcium, 10 µM picrotoxin, and 10 µM CNQX to isolate NMDA conductances.

All recording pipette solutions were made with deionized distilled water (resistance >18 MΩ cm^{-2}; Milli-Q system). Data were analyzed initially with Clampfit (v9) (Axon Instruments) and further processed and presented with Origin 6.1 (Microcal Software) and CorelDraw 10.0 (Corel) programs.

Novel Object Recognition (NOR)

Experiments were conducted as described previously (Hirst et al., 2006). Rats were habituated to the NOR test box twice a day for 2 consecutive days prior to testing. Each habituation session was comprised of a 3-minute exposure to the empty test box (46 x 30 x 45 cm), followed by 1 minute in the side annex (1 x 30 x 45 cm) and a further 3 minutes in the test box, thereby mimicking the test protocol. A vehicle dose was administered prior to one of the habituation sessions on each habituation day. The NOR test comprised 2 test sessions, T1 and T2, each lasting 3 minutes. On the first test day, T1, rats were habituated to the empty test box for 3 minutes and then placed in the side

annex for approximately 1 minute whilst 2 identical test objects were placed in the test arena equally spaced to each other and the side walls. The rat was then returned to the test arena and allowed to freely explore the objects for a further 3 minutes. At the end of the test session, the rat was returned to its home cage. Following a 24-hour inter-trial interval, the recall trial (T2) was conducted. T2 was similar to T1 except that one of the "familiar" objects was substituted for a novel one of a similar size and color but different shape. The objects used were made of black hardened plastic and were geometric shapes (towers and pyramids) that were of no relevance to the animals. Objects were cleaned between trials with 70% ethanol to eliminate odor cues.

T1 and T2 trials were recorded by GeoVision surveillance camera software and files were saved on DVD for remote scoring by an operator blinded to the treatments. Exploration was scored as time spent sniffing or licking the objects, when the nose was in contact with the object and was moving (i.e., when the animal was sniffing). Sitting on the object or next to it with the nose directed away was not classed as exploration. The discrimination index [(time spent exploring the novel object - time spent exploring the familiar object)/total exploration time] was then calculated for T2.

For the NYX-2925 groups, 0.01, 0.1, or 1 mg/kg p.o. was administered 60 minutes before T1 and CMC saline administered 1 hour before T2. For the SB399885 group, 10 mg/kg p.o. was administered 240 minutes before both T1 and T2. For the vehicle group, CMC saline (1 mL/kg) was administered 60 minutes before both T1 and T2.

Ultrasonic Vocalization (USV) Assay

Heterospecific rough-and-tumble play was conducted as previously described (Burgdorf et al., 2011b). The experimenter was blind to the treatment condition of the animals. Animals received 3 minutes of heterospecific rough-and-tumble play consisting of alternating 15-second blocks of heterospecific play and 15 seconds of no stimulation. High-frequency USVs were recorded and analyzed by sonogram in a blind manner as described previously (Burgdorf et al., 2011b). At the end of the 3-minute session, the latency for the rat to approach the experimenters hand to self-administer heterospecific play was also measured. Animals were not habituated to play stimulation before dosing and testing. Using this paradigm, the increase in 50-kHz USVs that occurs across trial blocks reflects positive emotional learning (Burgdorf et al., 2011b; Ishiyama and Brecht, 2016).

Animals were administered NYX-2925 (1 mg/kg p.o.) or CMC saline (p.o.) 1 hour before testing. Rats received the NMDA receptor glutamate site antagonist CPP (10 mg/kg i.p.) or sterile saline (i.p.) 2 hours before NYX-2925 (1 mg/kg p.o.) or CMC saline (p.o.). This dose of NYX-2925 was chosen given that it leads to CSF exposures that activate all 4 NMDAR subtypes (Figures 2A-D and 4A) and showed maximal facilitation of learning and memory in the novel object recognition test (Figure 5A).

Rota-Rod Test of Motor Coordination

Rota-Rod testing was conducted as previously described (Nadeson et al., 2002) using a 4-station Rota-Rod apparatus (Med Associates). One day before testing, animals received 3 Rota-Rod habituation sessions with at least 30 minutes between each session and an additional habituation session immediately before dosing (0 min). Animals were dosed with NYX-2925 (1–100 mg/kg p.o.) or CMC saline. Animals were tested 15, 30, 60, and 120 minutes using a within-subjects design. Habituation and testing consisted of placing rats onto the fixed speed version of the Rota-Rod test (16 RPM) for 300 seconds, and the latency to fall off the Rota-Rod was recorded.

Open Field Test of Locomotor Activity

Open field testing was conducted as previously described (Burgdorf et al., 2013). Rats were placed into the center chamber of the open field (40x40x20 cm) for 10 minutes under dim-red lighting 1 hour post dosing with NYX-2925 (1 mg/kg p.o.) or vehicle (1 mL/kg p.o.). Line crosses were scored offline from video recordings by an experimenter blinded to the treatment condition.

Drug Discrimination

Testing was conducted as described previously (Burgdorf et al., 2013). Adult male Sprague-Dawley rats were trained to discriminate ketamine (5.6 mg/kg, i.p.) from saline (1 mL/kg, i.p.) 5 d/wk (Monday-Friday; 15 min/d) in standard 2-lever operant conditioning chambers (Med Associates) under a double-alternation schedule of ketamine or saline (K, K, S, S, K, K, etc.). Rats were placed in the operant conditioning chamber 10 minutes post-injection and the session initiated as signaled by illumination of the chamber house light. Completion of 10 consecutive responses (fixed ratio 10; FR 10) on the correct lever resulted in delivery of a 45-mg food pellet (Bio-Serv) and illumination of a white stimulus light over the lever. Incorrect responding reset the FR for correct-lever responding. Food (Harlan Teklad Rodent Diet) access beyond those obtained during behavioral sessions was restricted to ~20 g given post session. Animals were tested following administration of various doses of NYX-2925 (1, 10, 100 mg/kg, p.o.), CMC saline (2 mL/kg) or ketamine (10, 17 30 mg/kg, p.o.), and lever selection and rates of responding were recorded. Doses of NYX-2925 and its vehicle were administered 1 hour prior to the session start and p.o. ketamine was administered 15 minutes prior to session start. For all p.o. test sessions, rats were also administered i.p. saline, 1 mL/kg, 10 minutes prior to session start to mimic training conditions. Training continued under the double alternation of 5.6 mg/kg ketamine and saline injections between test sessions. Illumination of lights, recording of responses, and pellet delivery were performed with MED-PC operant conditioning software (version 1.1).

Statistical Analysis

Behavioral and electrophysiological data were analyzed by ANOVA, followed by Fisher's PLSD posthoc test (Statview). The level of statistical significance was set at $P < .05$.

Data from the [^{3}H] MK-801 potentiation assay data was analyzed by Prism (Graphpad).

Results

[^{3}H] MK-801 Potentiation and Off-target Receptor Binding

NYX-2925 facilitated [^{3}H] MK-801 binding in all four human NMDAR2 subtypes. The concentration-response curves for NYX-2925 assessed in hNR1-expressing HEK cells transfected with hNR2A, 2B, 2C, and 2D are shown in Figure 2. The activity of NYX-2925 was 40.6%, 47.1%, 63.1%, and 57.8% of [^{3}H] MK-801 activity measured in the presence of maximal glycine for hNR2A, 2B, 2C, and 2D receptors, respectively. The potency (EC_{50}) of NYX-2925

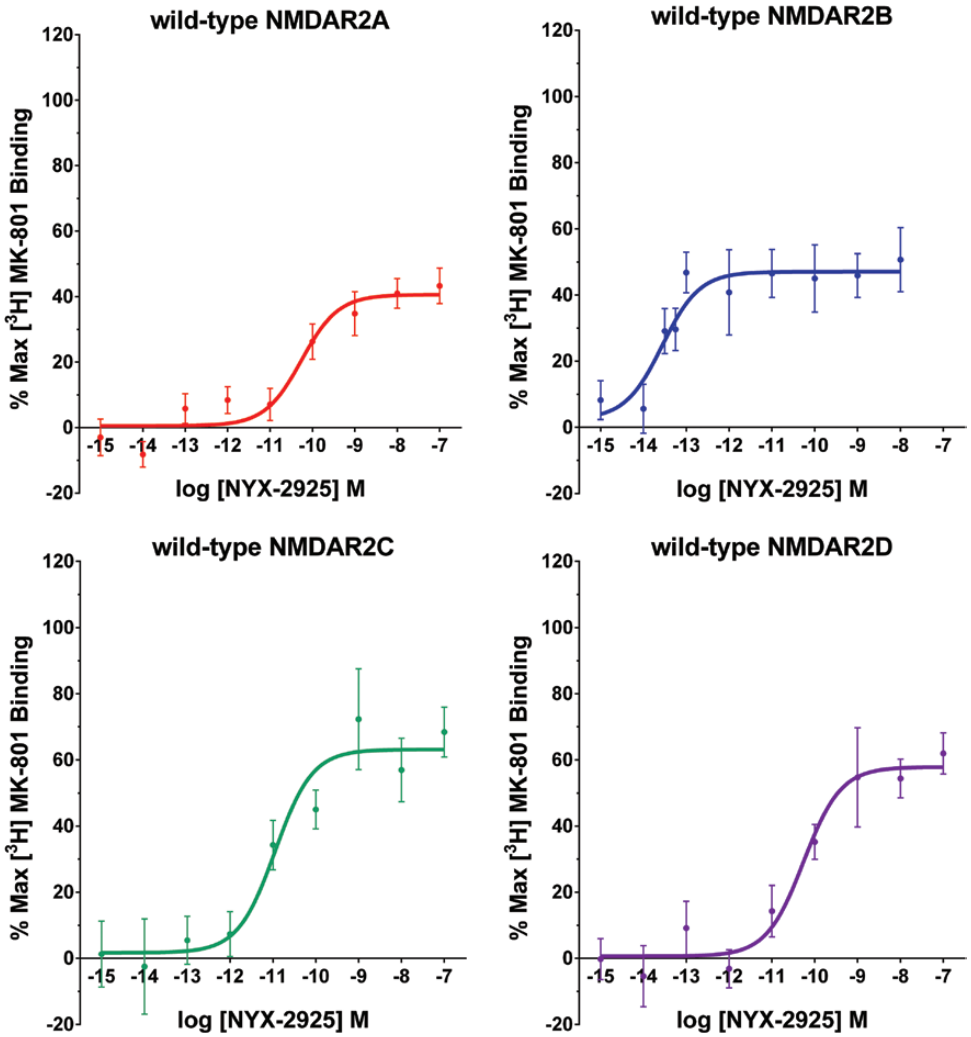

Figure 2. NYX-2925 is active at all 4 human N-methyl-D-aspartate receptor (hNMDAR) 2 subtypes. Potentiation of [^{3}H] MK-801 binding by NYX-2925 and glycine in hNMDAR subtype-expressing human embryonic kidney (HEK) cells. Stable hNMDAR1-expressing HEK cells were transiently transfected with cDNAs encoding hNMDAR2A, hNMDAR2B, hNMDAR2C, or hNMDAR2D. At 48 hours post-transfection, membrane-bound receptors were isolated, and the functional glycine site agonist effects were measured using the [^{3}H] MK-801 potentiation assay, as described in Methods. The percent maximal effects were calculated relative to stimulation in the presence of 1 mM glycine and 50 µM glutamate. Binding curves were fitted using GraphPad Prism software.

was 55 pM, 28 fM, 11 pM, and 55 pM for hNR2A, 2B, 2C, and 2D receptors, respectively.

NYX-2925 (10 µM) did not exhibit any significant affinity (considered >50%) for any of the 81 binding sites tested (Table 1). At 10 µM, NYX-2925 did not demonstrate significant inhibition or stimulation (agonism) in any of the 81 sites. This study provides evidence that NYX-2925 has a low potential for "off-target" activity.

NMDAR Current and Long-Term Potentiation in Hippocampus and Medial Prefrontal Cortex

NYX-2925 (100–500 nM) increased the magnitude of pharmacologically isolated NMDA current in Schaffer collateral-evoked EPSCs in CA1 pyramidal neurons (repeated-measures ANOVA $F_{(3,18)} = 7.2$, $P < .05$; within-subjects t test vs baseline NYX-2925 [100 and 500 nM] vs vehicle, $P < .05$; Figure 3A). NYX-2925 also increased the magnitude of LTP at Schaffer collateral-CA1 synapses ($F_{(4,30)} = 6.2$, $P < .05$; Fisher's PLSD posthoc test NYX-2925 [500 nM] vs vehicle, $P < .05$; Figure 3B) and inhibited LTD at these same synapses ($F_{(3,28)} = 4.1$, $P < .05$; Fisher's PLSD posthoc test NYX-2925 [5000 nM] vs vehicle, $P < .05$; Figure 3C). Moreover, LTP at mixed excitatory inputs synapsing in layer II/III of MPFC was also facilitated by NYX-2925 ($F_{(4,27)} = 5.6$, $P < .05$; Fisher's PLSD posthoc test NYX-2925 [100 and 500 nM] vs vehicle, $P < .05$; Figure 3D).

Pharmacokinetics and Toxicology

NYX-2925 showed high oral bioavailability, CNS penetration, and had a wide therapeutic index. As shown in Figure 4A, NYX-2925 (1 mg/kg p.o.) has a plasma Cmax of 706 nM at 1 hour, a plasma half-life of 6.8 hours, a CSF Cmax of 44 nM at 1 hour, and a CSF half-life of 1.2 hours. The Cmax CSF exposure is 44 nM. The oral bioavailability of NYX-2925 in plasma is 56% as calculated by the area under the curve of plasma exposure following 2 mg/kg i.v. or 10 mg/kg p.o. dosing (mean ± SEM AUC IV 2155.12 ± 45.77, p.o. 6053.73 ± 498.55 ng.h/mL).

The no observed adverse effect level of NYX-2925 for male Sprague Dawley rats when administered by the oral (gavage) route, once daily for 14 consecutive days is 1000 mg/kg/d as measured by mortality, clinical signs, body weight, food intake,

Table 1. Radioligand Displacement by NYX-2925 (10 μM)

Site	NYX-2925 % Inhibition
A1 (antagonist)	-4.2
A2A (agonist)	-6.1
A3 (agonist)	-4.9
α1 non-selective (antagonist)	-10
α2 non-selective (antagonist)	-11.6
β1 (agonist)	4.6
β2 (agonist)	-7.6
AT1 (antagonist)	-0.8
AT2 (agonist)	1.8
BZD central (agonist)	-9.1
BZD peripheral (antagonist)	-6.6
BB non-selective (agonist)	-9
B2 (agonist)	-3.1
CGRP (agonist)	3.6
CB1 (agonist)	5.7
CCK1 CCKA (agonist)	3.8
CCK2 CCKB (agonist)	-13
D1 (antagonist)	-19.9
D2S (antagonist)	6.8
D3 (antagonist)	-5.2
D4.4 (antagonist)	-5
D5 (antagonist)	4.1
ETA (agonist)	5.7
ETB (agonist)	1.3
GABA non-selective (agonist)	-18.8
GAL1 (agonist)	3
GAL2 (agonist)	3.7
PDGF (agonist)	-2.6
CXCR2 IL-8B (agonist)	-4.5
CCR1 (agonist)	0
TNF-α (agonist)	-21.7
H1 (antagonist)	2.4
H2 (antagonist)	0.5
MC4 (agonist)	3.4
MT1 ML1A (agonist)	1.4
M1 (antagonist)	-23.4
M2 (antagonist)	-6.1
M3 (antagonist)	-10.1
M4 (antagonist)	-11.3
M5 (antagonist)	5.6
NK1 (agonist)	-22.5
NK2 (agonist)	2.4
NK3 (antagonist)	-7.7
Y1 (agonist)	-3.4
Y2 (agonist)	-9.9
NTS1 / NT1 (agonist)	-11.4
δ2 (DOP) (agonist)	-4.2
κ (KOP) (agonist)	0.1
μ (MOP) (agonist)	-4.5
NOP / ORL1 (agonist)	5.9
PAC1 / PACAP (agonist)	-4.4
PPARγ (agonist)	-10.7
PCP (antagonist)	-5.7
EP2 (agonist)	4.7
EP4 (agonist)	7.5
IP PGI2 (agonist)	-5.1
P2X (agonist)	16.1
P2Y (agonist)	5.1
5-HT1A (agonist)	2.5
5-HT1B (antagonist)	-6.7
5-HT2A (antagonist)	-5.8
5-HT2B (agonist)	2.1
5-HT2C (antagonist)	-5.9
5-HT3 (antagonist)	2.7
5-HT5a (agonist)	-7.5
5-HT6 (agonist)	-8.6
5-HT7 (agonist)	-5.1
Sigma (non-selective) (agonist)	-15.8
SSST (non-selective) (agonist)	-13.8
GR (agonist)	-6.2
VPAC1 (VIP1) (agonist)	7.4
V1 a (agonist)	15.3
Verapamil site (antagonist)	3.4
hERG [3H] Dofetilide	-3
KV channel (antagonist)	-7.4
SKCa channel (antagonist)	5
Na+ channel (site 2) (antagonist)	7.3
Cl- channel GABA-gated (antagonist)	5.2
Norepinephrine transporter (antagonist)	-6.2
Dopamine transporter (antagonist)	-6.4
5-HT transporter (antagonist)	-13.9

Results that show an inhibition or stimulation >50% are considered to represent significant effects of the test compound.

and gross histopathology as well as organ weights. The plasma exposure (area under the curve) of NYX-2925 following 14 daily doses of 1000 mg/kg was 1074478 ng.h/mL compared with 494 ng.h/mL for a single behaviorally efficacious dose of 1 mg/kg, thus resulting in a projected therapeutic index of 2175.

Structural Plasticity

NYX-2925 (1 mg/kg p.o.; 24 hours post dosing) induced structural plasticity as indexed by increased diameter of spine heads ($F_{(1,3441)}=44.2$, $P<.05$) and necks ($F_{(1,3441)}=27.2$, $P<.05$) in the primary apical dendrites of dentate granule neurons (Figure 4B). Spine length ($F_{(1,3441)}=2.9$, $P>.05$) or total spine number ($F_{(1,65)}=1.1$, $P>.05$) was not affected by NYX-2925 (Figure 4B).

Metaplasticity

NYX-2925 persistently enhanced LTP at 24 hours and 1 week following a single dose (1 mg/kg p.o.) at Schaffer collateral-CA1 synapses after 3 submaximal high-frequency stimulus trains (2×100 Hz/800 ms, arrows). LTP was evaluated either 24 hours post dosing ($F_{(1,13)}=5.5$, $P<.05$) or 1 week post dosing ($F_{(1,14)}=8.8$, $P<.05$) as shown in Figure 4C-D.

Learning and Memory Tests

NYX-2925 facilitated learning and memory in multiple paradigms across a wide dose range. NYX-2925 (0.01, 0.1, 1 mg/kg p.o.), delivered 1 hour prior to T1, increased novel object recognition after a 24-hour delay between training and testing to a similar degree as the positive control SB399885, delivered 4 hours prior to T1 and T2 ($F_{(4,54)}=11.5$, $P<.05$; Fisher's PLSD post-hoc test NYX-2925 [0.01, 0.1, 1 mg/kg] or SB399885 vs vehicle, $P<.05$; Figure 5A).

NYX-2925 (1 mg/kg p.o.) facilitated positive emotional learning and this effect was blocked by pretreatment with a single dose of the NMDAR antagonist CPP as measured by both increased rates of hedonic 50-kHz USVs across trials

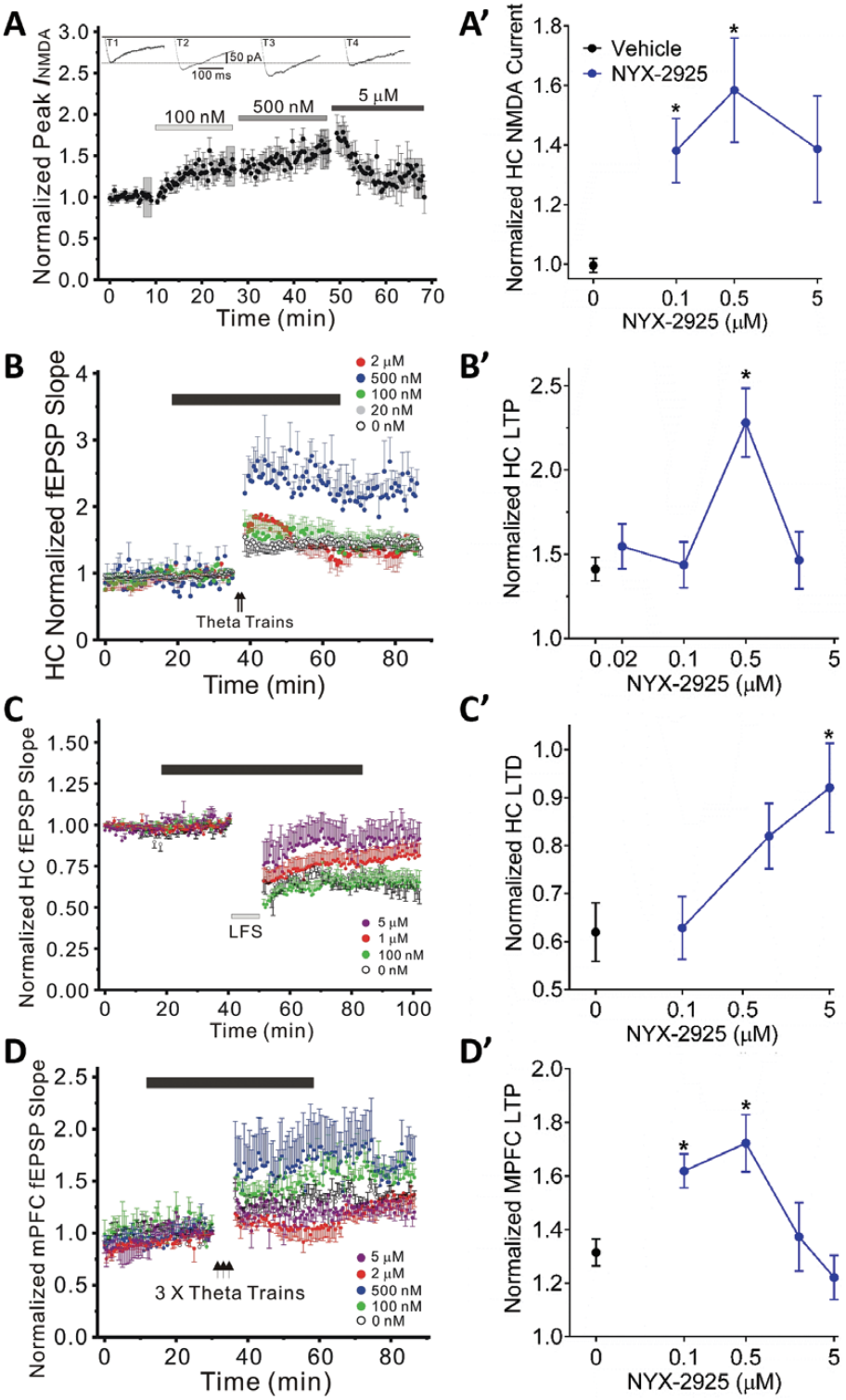

Figure 3. NYX-2925 facilitates NMDA current and NMDA receptor-dependent LTP, while decreasing LTD. (A) NYX-2925 (0.1–0.5 μM) enhanced the pharmacologically-isolated NMDAR current in Schaffer collateral-evoked EPSCs in hippocampal CA1 pyramidal neurons. NYX-2925 (B) enhanced the magnitude of LTP at 0.5 μM and (C) decreased the magnitude of LTD at 5 μM of synaptic transmission at Schaffer collateral-CA1 synapses as compared to untreated control (aCSF) slices. (D) NYX-2925 (0.1 and 0.5 μM) enhanced the magnitude of LTP in layer II/III-evoked normalized field EPSP slopes in rat slices recorded in MPFC layer IV. NYX-2925 was bath applied for 40–50 min starting 20 min before high-frequency theta trains to induce LTP (solid bar) or low-frequency stimulation to elicit LTD (solid bar). LTP/LTD was measured 40 min after high- or low-frequency stimulation. Data are shown as mean ± SEM. N = 7 cells per group (A) or 5–10 slices per group (B-D). * $P < .05$, (A) within-subjects *t* test vs baseline (B-D) Fishers PLSD post hoc test vs vehicle.

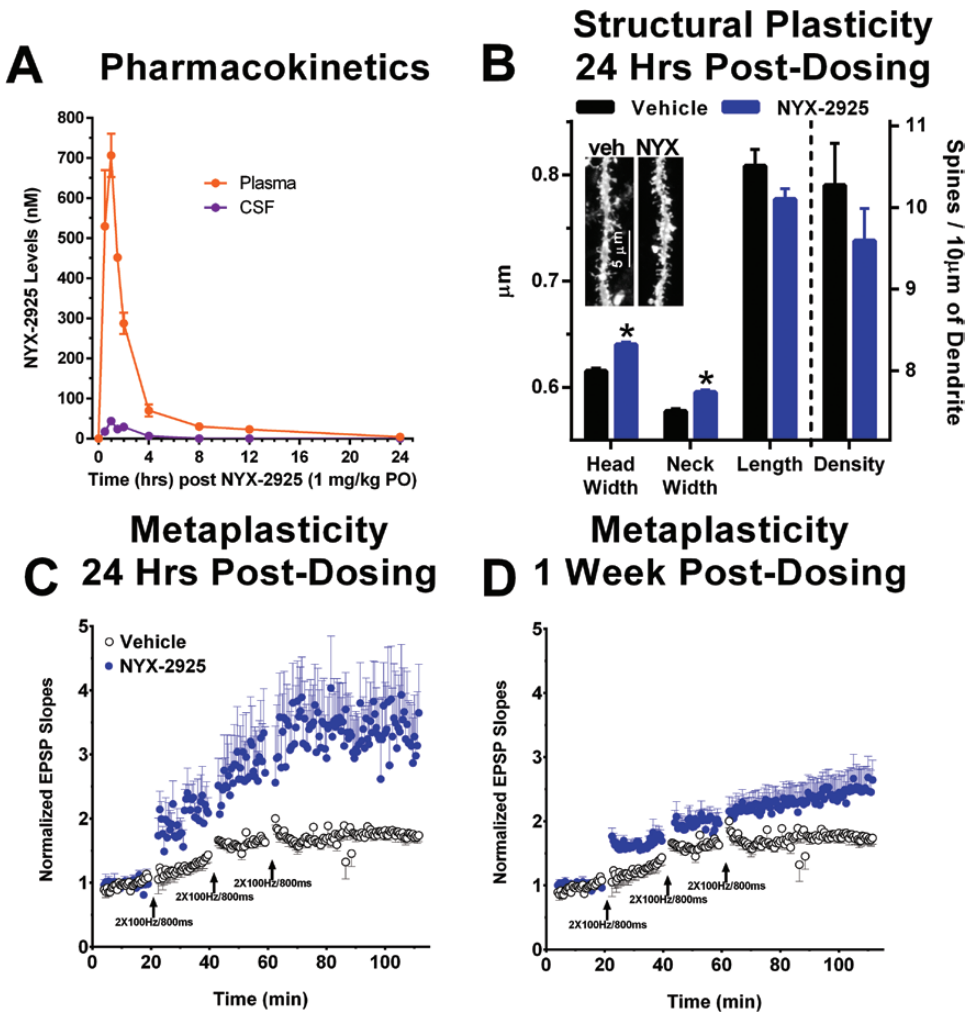

Figure 4. NYX-2925 persistently enhances hippocampal structural plasticity and metaplasticity following a single *in vivo* dose (1 mg/kg PO). (A) Plasma and CSF levels following dosing with NYX-2925 (1 mg/kg PO) were measured by LC/MS/MS. The C_{max} in the CSF is 44 nM (at 30 min post-dosing) which is well above the threshold for activing NR2A-D receptors (1 nM) as shown in Figure 2. A single *in vivo* dose of NYX-2925 (1 mg/kg PO) increased (B) spine head and neck diameter in hippocampal dentate gyrus primary dendrites 24 hrs post-dosing, and (C,D) the magnitude of LTP compared to slices from vehicle-treated control rats prepared (C) 24 hrs and (D) 1 week post-dosing (NYX-2925, 1 mg/kg PO) at Schaffer collateral-CA1 synapses after 3 sub-maximal high-frequency stimulus trains (2 × 100 Hz/800 ms, arrows). Data are shown as Mean ± SEM. N = (A) 2–3 rats, (B) 1412–2034 spines, and (C-D) 6–8 slices per group.

(repeated-measures ANOVA: dosing group $F_{(3,31)}=37.7$, $P<.05$; trials $F_{(5,31)}=39.8$, $P<.05$, dosing group x trials $F_{(15,31)}=15.0$, $P<.05$, Fisher's PLSD posthoc test NYX-2925 alone vs all other groups, $P<.05$; Figure 5B) and increased running speed to self-administer heterospecific rough-and-tumble play ($F_{(3,31)}=12.6$, $P<.05$; Fisher's PLSD posthoc test NYX-2925 alone vs all other groups, $P<.05$; Figure 5C). In addition, NYX-2925 (0.001–1 mg/kg p.o.) increased positive emotional learning 1 hour post dosing ($F_{(5,53)}=4.6$, $P<.05$, Fisher's PLSD posthoc test 0.001, 0.01, 0.1, 1 mg/kg vs vehicle, $P<.05$; data not shown).

Safety Pharmacology

NYX-2925 did no induce sedation/ataxia and does not show ketamine-like drug discrimination. NYX-2925 (1–100 mg/kg p.o.) did not induce a sedative/ataxic effect in the Rota-Rod test ($F_{(3,29)}=0.5$, $P>.05$; Figure 6A) or alter locomotor activity in the open field test at 1 mg/kg p.o. ($F_{(1,22)}=0.002$, $P>.05$; Figure 6B).

Ketamine (p.o.), but not NYX-2925, substituted for a training dose of ketamine (5.6 mg/kg i.p.) in a dose-dependent manner in the drug discrimination task ($F_{(6,36)}=90.9$, $P<.05$; Fisher's PLSD posthoc test ketamine [17 and 30 mg/kg p.o.] vs vehicle, $P<.05$; Figure 6C). Unlike ketamine, NYX-2925 did not suppress operant responding at the highest dose tested ($F_{(6,36)}=9.1$, $P<.05$; Fisher's PLSD post hoc test ketamine [30 mg/kg p.o.] vs vehicle, $P<.05$; Figure 6D)).

Discussion

The NMDA receptor has recently become an attractive target for the development of therapeutics for the treatment of a variety of CNS disorders. Clinical trial data have shown that NMDA receptor modulators have efficacy in mood disorders such as depression, obsessive compulsive disorder, schizophrenia, as well as in neuropathic pain, among others (Rodriguez et al., 2013; Cain et al., 2014; Feder et al., 2014; Fond et al., 2014; Maher et al., 2017). To date, only rapastinel and DCS have shown efficacy in clinical trials without the side effects seen with NMDA receptor antagonists. DCS has shown a comparatively weak therapeutic response profile and results have been mixed (Laake and Oeksengaard, 2002; Tuominen et al., 2005; Ori et al., 2015). Rapastinel is a peptide that must be

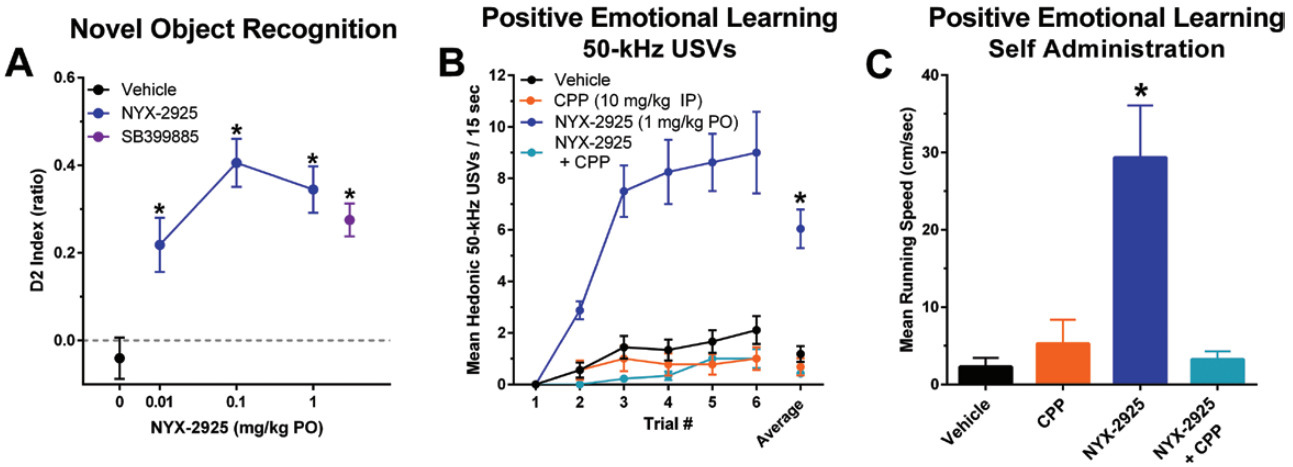

Figure 5. NYX-2925 facilitates learning and memory by activating NMDA receptors. (A) NYX-2925 (0.1–1 mg/kg PO, delivered 1 h prior to training) facilitated novel object recognition as measured by the D2 index [(novel object exploration time – familiar object exploration time) / total exploration time in T2)] tested 24 hrs after training. Pretreatment with a silent dose of the NMDA receptor antagonist CPP blocked the facilitation of learning in the positive emotional learning assay seen with NYX-2925 tested 1 hr after NYX-2925 administration (1 mg/kg PO) as measured by (B) increased rates of hedonic 50-kHz USVs across trial blocks and (C) increased running speed to self-administer heterospecific rough-and-tumble play. Data are shown as mean ± SEM. N = rats 8–12 per group. * $P < .05$, Fishers PLSD post hoc test (A) vs vehicle or (B) vs all other groups.

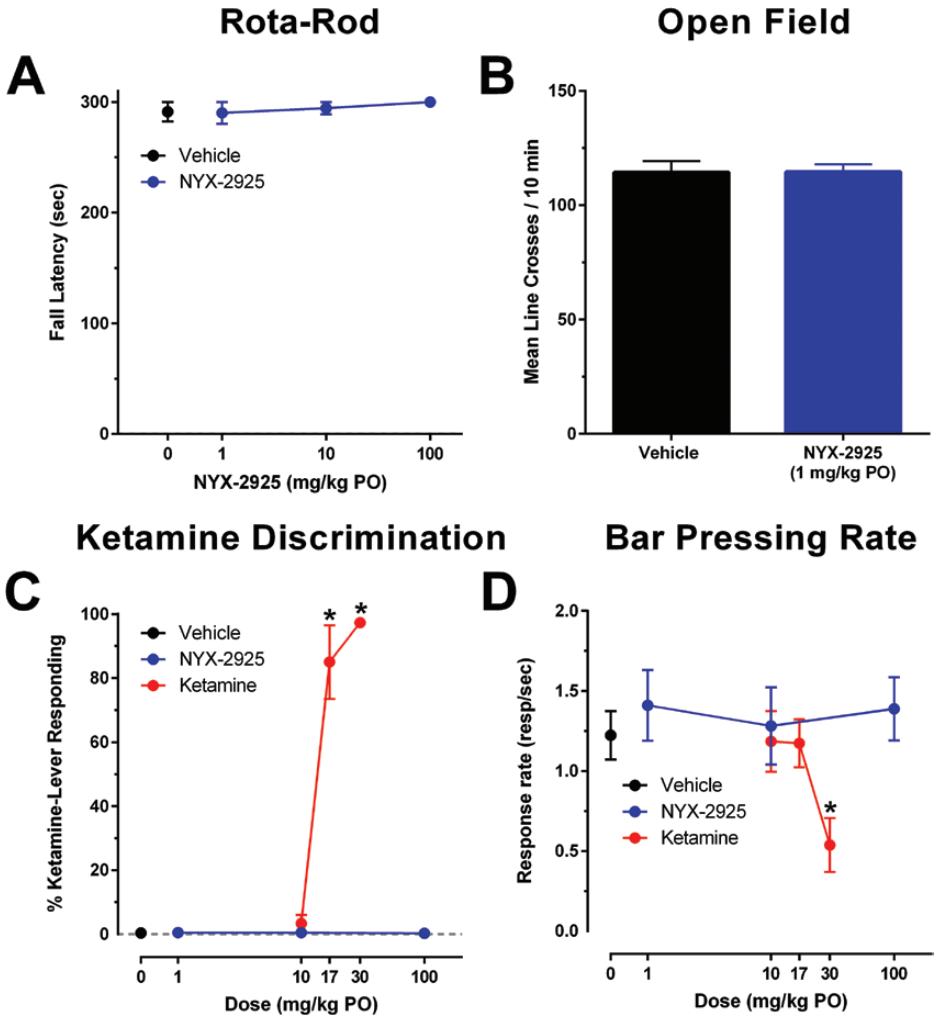

Figure 6. NYX-2925 does not produce ketamine-like sedative/ataxic or discriminative stimulus effects. (A) NYX-2925 (1, 10, 100 mg/kg PO) did not produce sedation/ataxia in the fixed speed (16 RPM) RotaRod test. (B) Locomotor activity in the open field was not altered by NYX-2925 (1 mg/kg PO). (C,D) NYX-2925 does not substitute for ketamine as measured by (C) percentage ketamine-lever responding and (D) rates of responding for ketamine (10, 17, 30 mg/kg PO) and NYX-2925 (1, 10, 100 mg/kg PO) in rats trained to discriminate 5.6 mg/kg ketamine from saline. N = 6–12 per group. * Fisher's PLSD post hoc test vs vehicle.

administered i.v. To obviate these problems, we developed a peptide mimetic program that uses spirocyclic-β-lactam chemistry to mimic the dipyrrolidine core of rapastinel.

The data reported here show that NYX-2925 is an NMDAR modulator that enhances activity-dependent synaptic plasticity in both the hippocampus and MPFC and facilitates learning and memory. This suggests that NYX-2925, like rapastinel (Moskal et al., 2017), operates through an NMDAR-triggered process that leads to lowering of the threshold for induction of LTP that results in enhancement of learning and memory, as well as long-term metaplasticity that persistently shifts the threshold for induction of LTP. In vivo, NYX-2925 facilitated novel object recognition and positive emotional learning, both of which are NMDAR-dependent learning tasks (Burgdorf et al., 2011b; van der Staay et al., 2011), and these effects were blocked by pretreatment with the NMDAR glutamate site antagonist CPP. Further, the dose used to facilitate learning in vivo (1 mg/kg p.o.) led to CSF drug levels that activate NR2A-D containing NMDARs in vitro, facilitate both NMDA current and NMDAR-dependent LTP in slices from hippocampus and MPFC, and reduce while actually reducing LTD in hippocampus. The observation that NYX-2925 shares with rapastinel an ability to simultaneously enhance the induction of LTP, while suppressing that of LTD (X. L. Zhang et al., 2008), is intriguing, given that studies have suggested that LTP and LTD may be preferentially induced by NMDARs containing NR2B and NR2A subunits, respectively (Bartlett et al., 2007; Morishita et al., 2007; Yashiro and Philpot, 2008). This leads us to conclude that NYX-2925, like rapastinel, may selectively activate NR2B-containing NMDARs (Zhang et al., 2008). In addition, NYX-2925 facilitated learning and memory, metaplasticity of LTP, and structural plasticity, 24 hours after a single dose, when NYX-2925 was no longer present in the CSF. Thus, NYX-2925 produces its behavioral effects by facilitating NMDAR-dependent plasticity acutely via direct activation of NMDAR and chronically by enhancing both metaplasticity and structural plasticity triggered by NMDAR activation.

NYX-2925 displays the properties of an attractive therapeutic for NMDAR-modulated CNS disorders. It operates through an NMDAR-triggered, AMPAR-dependent mechanism that leads to metaplasticity processes similar to LTP, which result in enhancements in learning and memory as well as long-term metaplasticity (Abraham and Bear, 1996). NYX-2925 is orally bioavailable and does not show ketamine-like side effects or observable adverse effects in toxicology studies, suggesting a wide therapeutic index (>1000).

Alonso et al. (2001) showed that spirocyclic β-lactams could be synthesized with β -turn conformations making the creation of peptidomimetics using conventional peptide chemistry techniques possible, and Bittermann and Gmeiner (2006) reported the synthetic methods for β-turn-containing spirocyclic-β-lactams starting from natural proline. Recently, this approach has been used to develop peptidomimetics of the dopamine receptor modulating peptide L-prolyl-L-leucyl-glycinamide (Khalil et al., 1999) and the creation of somatostatin mimetics (Lesma et al., 2013). Using a similar chemical synthesis approach, we have been able to create a novel platform of rapastinel mimetics, exemplified by NYX-2925 that may be useful tools to study NMDAR structure and function. And since NYX 2925 appears to be an excellent therapeutic candidate, other compounds from this platform may lead to additional NMDAR modulators with therapeutic potential.

Statement of Interest

P. K. Stanton is a consultant for Aptinyx, Inc. and has received financial compensation and stock. X.-L. Zhang is supported by a grant from Aptinyx, Inc., granted to P. K. Stanton. M. A. Khan, D. R. Houck, A. L. Gross, C. Cearley, T. M. Madsen, R. A. Kroes, J. S. Burgdorf, and J. R. Moskal are employees of Aptinyx, Inc., and have received financial compensation and stock.

Acknowledgments

The authors thank Puja Kansara, Elizabeth Pollard, Emma Rodriguez, and Mary Schmidt for their excellent technical assistance.

References

Abraham WC, Bear MF (1996) Metaplasticity: the plasticity of synaptic plasticity. Trends Neurosci 19:126–130.

Alonso E, Lopez-Ortiz F, del Pozo C, Peralta E, Macias A, Gonzalez J (2001) Spiro beta-lactams as beta-turn mimetics. Design, synthesis, and NMR conformational analysis. J Org Chem 66:6333–6338.

Bartlett TE, Bannister NJ, Collett VJ, Dargan SL, Massey PV, Bortolotto ZA, Fitzjohn SM, Bashir ZI, Collingridge GL, Lodge D (2007) Differential roles of NR2A and NR2B-containing NMDA receptors in LTP and LTD in the CA1 region of two-week old rat hippocampus. Neuropharmacology 52:60–70.

Bittermann H, Gmeiner P (2006) Chirospecific synthesis of spirocyclic beta-lactams and their characterization as potent type II beta-turn inducing peptide mimetics. J Org Chem 71:97–102.

Bliss TV, Collingridge GL (1993) A synaptic model of memory: long-term potentiation in the hippocampus. Nature 361:31–39.

Burgdorf J, Zhang XL, Weiss C, Matthews E, Disterhoft JF, Stanton PK, Moskal JR (2011a) The N-methyl-D-aspartate receptor modulator GLYX-13 enhances learning and memory, in young adult and learning impaired aging rats. Neurobiol Aging 32:698–706.

Burgdorf J, Kroes RA, Weiss C, Oh MM, Disterhoft JF, Brudzynski SM, Panksepp J, Moskal JR (2011b) Positive emotional learning is regulated in the medial prefrontal cortex by GluN2B-containing NMDA receptors. Neuroscience 192:515–523.

Burgdorf J, Zhang XI, Nicholson KL, Balster RL, Leander JD, Stanton PK, Gross AL, Kroes RA, Moskal JR (2013) GLYX-13, an NMDA receptor glycine-site functional partial agonist, induces antidepressant-like effects without ketamine-like side effects. Neuropsychopharmacology 38:729–742.

Burgdorf J, Kroes RA, Zhang XL, Gross AL, Schmidt M, Weiss C, Disterhoft JF, Burch RM, Stanton PK, Moskal JR (2015a) Rapastinel (GLYX-13) has therapeutic potential for the treatment of post-traumatic stress disorder: characterization of a NMDA receptor-mediated metaplasticity process in the medial prefrontal cortex of rats. Behav Brain Res 294:177–185.

Burgdorf J, Zhang XL, Weiss C, Gross A, Boikess SR, Kroes RA, Khan MA, Burch RM, Rex CS, Disterhoft JF, Stanton PK, Moskal JR (2015b) The long-lasting antidepressant effects of rapastinel (Glyx-13) are associated with a metaplasticity process in the medial prefrontal cortex and hippocampus. Neuroscience 308:202–211.

Burgdorf J, Colechio EM, Stanton P, Panksepp J (2017) Positive emotional learning induces resilience to depression: a role for NMDA receptor-mediated synaptic plasticity. Curr Neuropharmacol 15:3–10.

Cain CK, McCue M, Bello I, Creedon T, Tang DI, Laska E, Goff DC (2014) d-Cycloserine augmentation of cognitive remediation in schizophrenia. Schizophr Res 153:177–183.

Coyle JT (2012) NMDA receptor and schizophrenia: a brief history. Schizophr Bull 38:920–926.

Cull-Candy S, Brickley S, Farrant M (2001) NMDA receptor subunits: diversity, development and disease. Curr Opin Neurobiol 11:327–335.

Danysz W, Parsons CG (1998) Glycine and N-methyl-D-aspartate receptors: physiological significance and possible therapeutic applications. Pharmacol Rev 50:597–664.

de Kleine RA, Hendriks GJ, Kusters WJ, Broekman TG, van Minnen A (2012) A randomized placebo-controlled trial of D-cycloserine to enhance exposure therapy for posttraumatic stress disorder. Biol Psychiatry 71:962–968.

Dolino DM, Cooper D, Ramaswamy S, Jaurich H, Landes CF, Jayaraman V (2015) Structural dynamics of the glycine-binding domain of the N-methyl-D-aspartate receptor. J Biol Chem 290:797–804.

Feder A, Parides MK, Murrough JW, Perez AM, Morgan JE, Saxena S, Kirkwood K, Aan Het Rot M, Lapidus KA, Wan LB, Iosifescu D, Charney DS (2014) Efficacy of intravenous ketamine for treatment of chronic posttraumatic stress disorder: a randomized clinical trial. JAMA Psychiatry 71:681–688.

Fond G, Loundou A, Rabu C, Macgregor A, Lancon C, Brittner M, Micoulaud-Franchi JA, Richieri R, Courtet P, Abbar M, Roger M, Leboyer M, Boyer L (2014) Ketamine administration in depressive disorders: a systematic review and meta-analysis. Psychopharmacology (Berl) 231:3663–3676.

Ghasemi M, Phillips C, Trillo L, De Miguel Z, Das D, Salehi A (2014) The role of NMDA receptors in the pathophysiology and treatment of mood disorders. Neurosci Biobehav Rev 47:336–358.

Ghasemi M, Schachter SC (2011) The NMDA receptor complex as a therapeutic target in epilepsy: a review. Epilepsy Behav 22:617–640.

Goff DC (2012) D-cycloserine: an evolving role in learning and neuroplasticity in schizophrenia. Schizophr Bull 38:936–941.

Haring R, Stanton PK, Scheideler MA, Moskal JR (1991) Glycine-like modulation of N-methyl-D-aspartate receptors by a monoclonal antibody that enhances long-term potentiation. J Neurochem 57:323–332.

Harris RE, Sundgren PC, Pang Y, Hsu M, Petrou M, Kim SH, McLean SA, Gracely RH, Clauw DJ (2008) Dynamic levels of glutamate within the insula are associated with improvements in multiple pain domains in fibromyalgia. Arthritis Rheum 58:903–907.

Hirst WD, Stean TO, Rogers DC, Sunter D, Pugh P, Moss SF, Bromidge SM, Riley G, Smith DR, Bartlett S, Heidbreder CA, Atkins AR, Lacroix LP, Dawson LA, Foley AG, Regan CM, Upton N (2006) SB-399885 is a potent, selective 5-HT6 receptor antagonist with cognitive enhancing properties in aged rat water maze and novel object recognition models. Eur J Pharmacol 553:109–119.

Iacobucci GJ, Popescu GK (2017) NMDA receptors: linking physiological output to biophysical operation. Nat Rev Neurosci 18:236–249.

Ishiyama S, Brecht M (2016) Neural correlates of ticklishness in the rat somatosensory cortex. Science 354:757–760.

Karakas E, Furukawa H (2014) Crystal structure of a heterotetrameric NMDA receptor ion channel. Science 344:992–997.

Khalil EM, Ojala WH, Pradhan A, Nair VD, Gleason WB, Mishra RK, Johnson RL (1999) Design, synthesis, and dopamine receptor modulating activity of spiro bicyclic peptidomimetics of L-prolyl-L-leucyl-glycinamide. J Med Chem 42:628–637.

Laake K, Oeksengaard AR (2002) D-cycloserine for Alzheimer's disease. Cochrane Database Syst Rev:CD003153.

Lesma G, Cecchi R, Cagnotto A, Gobbi M, Meneghetti F, Musolino M, Sacchetti A, Silvani A (2013) Tetrahydro-beta-carboline-based spirocyclic lactam as type II' beta-turn: application to the synthesis and biological evaluation of somatostatine mimetics. J Org Chem 78:2600–2610.

Lu W, Du J, Goehring A, Gouaux E (2017) Cryo-EM structures of the triheteromeric NMDA receptor and its allosteric modulation. Science 355:pii: eaal3729.

Maher DP, Chen L, Mao J (2017) Intravenous ketamine infusions for neuropathic pain management: a promising therapy in need of optimization. Anesth Analg 124:661–674.

Matsuzaki M, Honkura N, Ellis-Davies GC, Kasai H (2004) Structural basis of long-term potentiation in single dendritic spines. Nature 429:761–766.

Millecamps M, Centeno MV, Berra HH, Rudick CN, Lavarello S, Tkatch T, Apkarian AV (2007) D-cycloserine reduces neuropathic pain behavior through limbic NMDA-mediated circuitry. Pain 132:108–123.

Morishita W, Lu W, Smith GB, Nicoll RA, Bear MF, Malenka RC (2007) Activation of NR2B-containing NMDA receptors is not required for NMDA receptor-dependent long-term depression. Neuropharmacology 52:71–76.

Morris RG (2013) NMDA receptors and memory encoding. Neuropharmacology 74:32–40.

Moskal JR, Burgdorf JS, Stanton PK, Kroes RA, Disterhoft JF, Burch RM, Khan MA (2017) The development of rapastinel (formerly GLYX-13); a rapid acting and long lasting antidepressant. Curr Neuropharmacol 15:47–56.

Moskal JR, Kuo AG, Weiss C, Wood PL, O'Connor Hanson A, Kelso S, Harris RB, Disterhoft JF (2005) GLYX-13: a monoclonal antibody-derived peptide that acts as an N-methyl-D-aspartate receptor modulator. Neuropharmacology 49:1077–1087.

Nadeson R, Tucker A, Bajunaki E, Goodchild CS (2002) Potentiation by ketamine of fentanyl antinociception. I. An experimental study in rats showing that ketamine administered by non-spinal routes targets spinal cord antinociceptive systems. Br J Anaesth 88:685–691.

Noguchi J, Matsuzaki M, Ellis-Davies GC, Kasai H (2005) Spine-neck geometry determines NMDA receptor-dependent Ca2+ signaling in dendrites. Neuron 46:609–622.

Ori R, Amos T, Bergman H, Soares-Weiser K, Ipser JC, Stein DJ (2015) Augmentation of cognitive and behavioural therapies (CBT) with d-cycloserine for anxiety and related disorders. Cochrane Database Syst Rev:CD007803.

Ota KT, Liu RJ, Voleti B, Maldonado-Aviles JG, Duric V, Iwata M, Dutheil S, Duman C, Boikess S, Lewis DA, Stockmeier CA, DiLeone RJ, Rex C, Aghajanian GK, Duman RS (2014) REDD1 is essential for stress-induced synaptic loss and depressive behavior. Nat Med 20:531–535.

Paoletti P, Bellone C, Zhou Q (2013) NMDA receptor subunit diversity: impact on receptor properties, synaptic plasticity and disease. Nat Rev Neurosci 14:383–400.

Parent MA, Wang L, Su J, Netoff T, Yuan LL (2010) Identification of the hippocampal input to medial prefrontal cortex in vitro. Cereb Cortex 20:393–403.

Patrizi A, Picard N, Simon AJ, Gunner G, Centofante E, Andrews NA, Fagiolini M (2016) Chronic administration of the N-methyl-D-aspartate receptor antagonist ketamine improves Rett Syndrome phenotype. Biol Psychiatry 79:755–764.

Preskorn S, Macaluso M, Mehra DO, Zammit G, Moskal JR, Burch RM, Group GCS (2015) Randomized proof of concept trial of GLYX-13, an N-methyl-D-aspartate receptor glycine site partial agonist, in major depressive disorder nonresponsive to a previous antidepressant agent. J Psychiatr Pract 21:140–149.

Pyke T, Osmotherly PG, Baines S (2016) Measuring glutamate levels in the brains of fibromyalgia patients and a potential role for glutamate in the pathophysiology of fibromyalgia symptoms: a systematic review. Clin J Pain 33:944–954.

Robb CM (1991) Restrictive covenant law in Georgia: back to the drawing board. J Med Assoc Ga 80:546–548.

Rodriguez CI, Kegeles LS, Levinson A, Feng T, Marcus SM, Vermes D, Flood P, Simpson HB (2013) Randomized controlled crossover trial of ketamine in obsessive-compulsive disorder: proof-of-concept. Neuropsychopharmacology 38: 2475–2483.

Rodriguez CI, Zwerling J, Kalanthroff E, Shen H, Filippou M, Jo B, Simpson HB, Burch RM, Moskal JR (2016) Effect of a novel NMDA receptor modulator, rapastinel (formerly GLYX-13), in OCD: proof of concept. Am J Psychiatry 173:1239–1241.

Tavoloni N, Schaffner F (1989) Bile secretory apparatus in the newborn dog: relationship between structural and functional immaturities. Biol Neonate 55:124–135.

Thompson LT, Moskal JR, Disterhoft JF (1992) Hippocampus-dependent learning facilitated by a monoclonal antibody or D-cycloserine. Nature 359:638–641.

Traynelis SF, Wollmuth LP, McBain CJ, Menniti FS, Vance KM, Ogden KK, Hansen KB, Yuan H, Myers SJ, Dingledine R (2010) Glutamate receptor ion channels: structure, regulation, and function. Pharmacol Rev 62:405–496.

Tuominen HJ, Tiihonen J, Wahlbeck K (2005) Glutamatergic drugs for schizophrenia: a systematic review and meta-analysis. Schizophr Res 72:225–234.

van der Staay FJ, Rutten K, Erb C, Blokland A (2011) Effects of the cognition impairer MK-801 on learning and memory in mice and rats. Behav Brain Res 220:215–229.

Vasilescu AN, Schweinfurth N, Borgwardt S, Gass P, Lang UE, Inta D, Eckart S (2017) Modulation of the activity of N-methyl-d-aspartate receptors as a novel treatment option for depression: current clinical evidence and therapeutic potential of rapastinel (GLYX-13). Neuropsychiatr Dis Treat 13:973–980.

Wilkinson D, Wirth Y, Goebel C (2014) Memantine in patients with moderate to severe Alzheimer's disease: meta-analyses using realistic definitions of response. Dement Geriatr Cogn Disord 37:71–85.

Yashiro K, Philpot BD (2008) Regulation of NMDA receptor subunit expression and its implications for LTD, LTP, and metaplasticity. Neuropharmacology 55:1081–1094.

Zhang L, Xu T, Wang S, Yu L, Liu D, Zhan R, Yu SY (2013) NMDA GluN2B receptors involved in the antidepressant effects of curcumin in the forced swim test. Prog Neuropsychopharmacol Biol Psychiatry 40:12–17.

Zhang XL, Sullivan JA, Moskal JR, Stanton PK (2008) A NMDA receptor glycine site partial agonist, GLYX-13, simultaneously enhances LTP and reduces LTD at Schaffer collateral-CA1 synapses in hippocampus. Neuropharmacology 55:1238–1250.

Zhou HY, Chen SR, Pan HL (2011) Targeting N-methyl-D-aspartate receptors for treatment of neuropathic pain. Expert Rev Clin Pharmacol 4:379–388.